96-3655

Spacecraft Autonomous Navigation for Formation Flying Earth orbiters Using GPS

Joseph R. Guinn[1]
Ronald J. Boain[2]

This paper extends earlier analysis for autonomous orbit determination and control of Earth orbiting spacecraft. The earlier analysis was limited to a single spacecraft with a ground track repeat requirement [1]. This work shows that a similar technique is applicable for two spacecraft flying in formation. Tracking and orbit determination functions are performed using the Global Positioning System (GPS). Orbit control is performed by using a simple empirical strategy to infer absolute and relative orbit decay and subsequently provide orbit adjustment information. Simulation results and a proposed strategy are provided for the New Millennium Earth Orbiter- 1 autonomous formation flying mission.

INTRODUCTION

One of the key technologies to be used extensively on future Earth orbiting missions is autonomous navigation. By navigation here, it is meant that process of determining and controlling the trajectory or orbit of a spacecraft during its mission in a manner consistent with the mission and navigation requirements. Autonomous, in this context, relates to a state of self-contained sensing, judging, and decision making to empower actions on the spacecraft without outside advice or intervention. Thus, autonomous navigation is navigation done by a spacecraft based on capabilities resident within that spacecraft and without ground intervention.

Single spacecraft autonomous navigation has been proposed [1-4] and partially validated for various mission scenarios **[5-6].** Within autonomous navigation, there are several possible "control objectives" for trajectory or orbit adjustments dictated by the navigation requirements and implemented principally within the decision and maneuver functions of an autonomous navigation system. Two or more spacecraft in Earth orbit actively preserving, within limits, some geometrical alignment is just one. of the possible control objectives achievable within the context of autonomous navigation. This would be formation flying. In its simplest form, two spacecraft control and maintain their dynamic states with respect to one another according to some prespecified requirement, usually expressed as a nominal separation distance and a control band on that separation. The characteristics of this prespecified requirement, as a first order factor, determine the complexity of algorithms and the difficulty of the overall autonomous navigation implementation such that large distances and tight control bands are more difficult and Costly.

---

[1] Navigation and Flight Mechanics Section at the Jet Propulsion Laboratory, California Institute of Technology, 4800 Oak Grove Drive Pasadena, California 91109, (818) 354-042S, AIAA Member

[2] Missions and Systems Architecture Section at the Jet Propulsion Laboratory, California Institute of Technology, 4800" Oak Grove Drive Pasadena, California 91109, (818) 354-5 12?

For the New Millennium Earth Orbiter-1 (EO-1) mission the problem is to make EO-1 fly in formation ahead of the Landsat-7 (LS-7) satellite. Formation flying here is required in order to take coordinated, co-registered images of reference geographic sites for a scientific comparison of the two imaging systems. in this mode of operation, the relative positions of EO-1 and LS-7 will be maintained and controlled with respect to one another according to the mission requirement for "simultaneity" of measurements. The separation distance between EO-1 and LS-7 (though not yet determined as a specific requirement) can be as great as 6750 km and still provide adequate science But much smaller separations are desirable and easily achieved with the autonomous navigation technology presently available. Equally important, a control band size on the order of 230 km or less seems desirable and attainable within this same technology. (This is based on the current mission concept where LS-7 executes its nominal mission as a non-cooperative partner with EO-1, except perhaps to share its mission plan and navigational data at Orbit Maintenance Maneuvers. Smaller control bands are possible if some form of cooperative, near real-time data exchange were possible between EO-1 and LS-7, thus providing a more rigorous demonstration of formation flying.) Cooperative formation flying using various methods of filtering spacecraft to spacecraft range have been proposed [7-9].

Elements of this autonomous navigation system, shown in Fig.1, include: Global Positioning System (GPS) tracking and orbit determination, maneuver decision, maneuver design, and maneuver implementation. This paper describes each element and provides preliminary simulation results for the New Millennium EO-1 / LS-7 autonomous navigation formation flying technology validation mission.

GPS TRACKING

Several spaceborne GPS receivers have been developed to track GPS signals from low Earth orbit [10]. These multiple channel receivers provide the capability to collect GPS pseudorange and carrier phase observations along with navigational data [11] simultaneously from a minimum of four satellites. Most receivers operate by tracking many more than the minimum. Generally, a single omnidirectional antenna is used; however, multiple antennae may be employed to allow for attitude measurement, increased antenna gain, or to avoid signal blockage due to spacecraft attitude maneuvering.

Dual frequency observations provide for ionospheric delay elimination. However, only single frequency observations are available for civilian use. Single frequency "codeless" techniques are now available in some GPS receivers to allow for ionosphere calibration without requiring special security agreements [12].

Fig. 1- Autonomous Navigation Formation Flying System for New Millennium EO-1 Mission

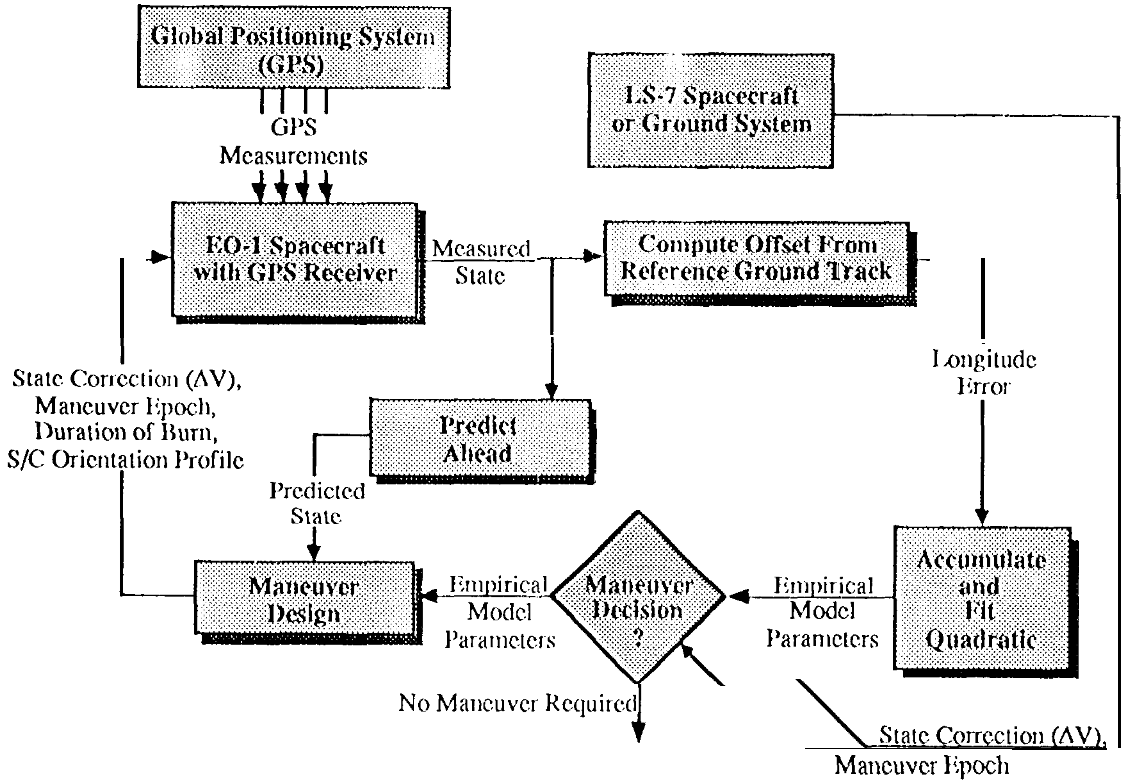
Global Positioning System (GPS)
GPS Measurements
LS-7 Spacecraft or Ground System
EO-1 Spacecraft with GPS Receiver
Measured State
Compute Offset From Reference Ground Track
State Correction (ΔV), Maneuver Epoch, Duration of Burn, S/C Orientation Profile
Longitude Error
Predict Ahead
Predicted State
Accumulate and Fit Quadratic
Maneuver Design
Empirical Model Parameters
Maneuver Decision ?
Empirical Model Parameters
No Maneuver Required
State Correction (ΔV), Maneuver Epoch

ORBIT DETERMINATION

Autonomous real-time orbit determination is available using only GPS tracking data. The GPS provides two levels of service: a Standard Positioning Service (SPS), available to all users on a continuous, world wide basis with no direct charge and an encoded Precise Positioning Service (PPS) intended primarily for military use. SPS is intentionally degraded with a process called Selective Availability (SA) [13] and has an advertised positioning accuracy of 100 meters horizontal and 140 meters vertical (95 percent probability) [14].

Orbit accuracy improvements to the S1'S service can be obtained by employing user spacecraft dynamic models and an extended Kalman filter. An initialization or settling period is required to obtain the needed apriori constraints. Afterward, real-time orbit solutions are available. Improved accuracy at the expense of increased complexity may not justify its use for a non-cooperative formation flying mission such as EO-1. However, for future cooperative and/or tight separation control missions, this form of orbit determination may be required.

Fig.2 - GPS Derived TOPEX/Poseidon Orbit Determination Results

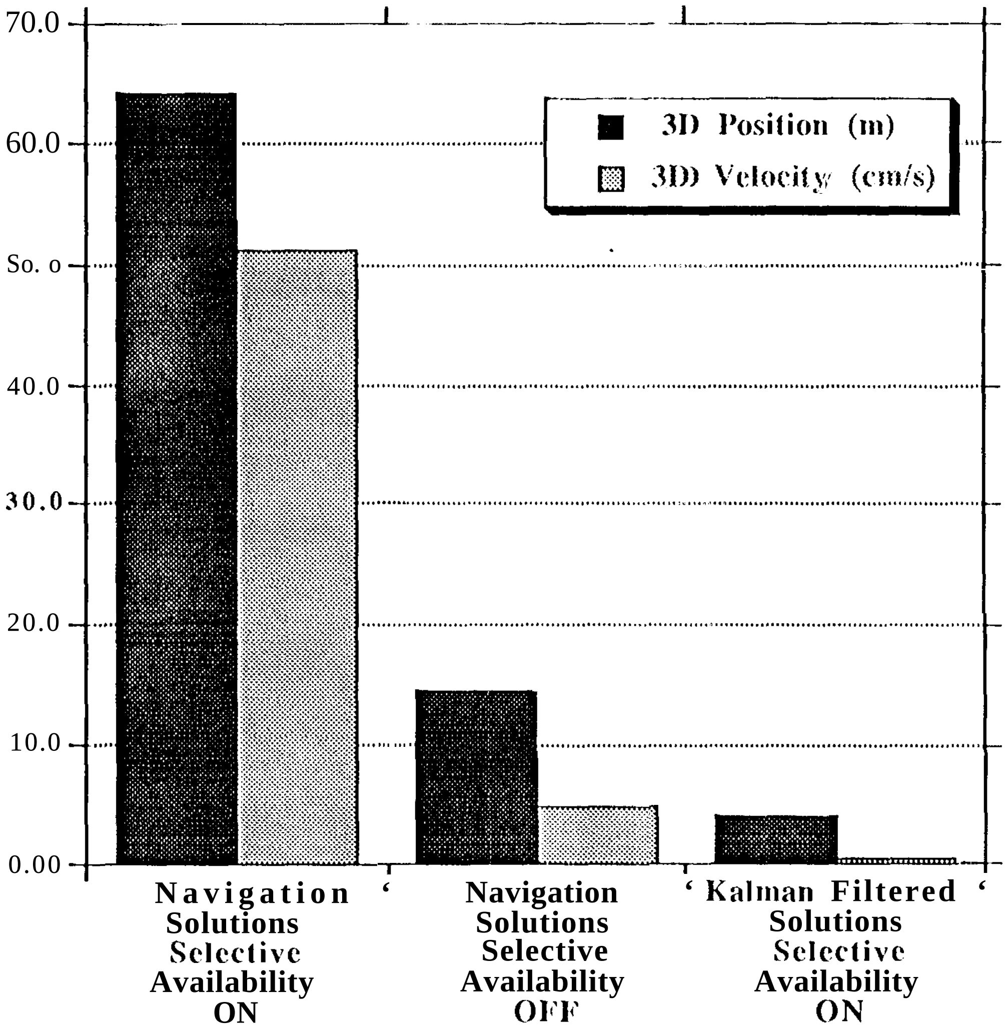

Fig.2 provides a summary of actual orbit determination accuracies achieved using TOPEX/Poseidon GPS flight receiver observations. In order to evaluate the orbit determination performance for the various tracking modes shown, a "near-truth" orbit solution was required, This "near-truth" orbit solution, also called a Precision orbit Ephemeris (POE), **was** computed using single frequency carrier phase and pseudorange observations from TOPEX/Poseidon and 15 globally distributed ground stations. It is a differential solution with full dynamic modeling and batch/sequential parameter estimation over a 30-hour arc. Stochastic white noise clocks and carrier phase biases were estimated along with the spacecraft state to produce an orbit accurate to about 15 cm total position. More details regarding the accuracy and production of this GPS based POE can be found in Ref. 15.

In Fig.2, the result "Navigation Solutions SA ON", was derived by computing the RMS (over 24 hours at 5 minute samples) of the total position differences between the onboard "navigation solutions" and the POE. The 64 m total position error is consistent with results expected under SPS with SA ON. Other spaceborne GPS missions have produced similar "navigation solution" performance [16-19].

The second result, "Navigation Solutions SA OFF", was computed the same as the first but for a different day when no SA clock manipulation was apparent. As expected the orbit accuracy improved to a total position error of about 15 m.

The final result shows what can be obtained by using an extended Kalman filter along with modelling the satellite dynamics. The result, "Kalman Filtered Solutions SA ON", achieved an accuracy of about 5 m after a settling time of approximately 4 hours. For lower altitudes the dynamic modelling errors are expected to increase; however, orbit accuracies are still expected to be below 10 m. Dynamic models used were: Sun and Moon n-body, 50x50 JGM3 geopotential, DTM drag model, solar anti Earth radiation pressure, and solid earth tides. The extended Kalman filter is defined here as a sequential processing of the available observations with state and nominal trajectory updates at each epoch. By utilizing stochastic clock estimation, accumulating the UD information matrix and exploiting the high fidelity dynamic models, orbit accuracies are improved and maintainable. Thus, once initialized/settled the extended Kalman filter produces more accurate orbit determination results than the kinematic (non-dynamic) "navigation solutions".

For non-cooperative formation flying, orbit determination performance is not required to be as accurate. This results from the fact that routine orbit determination of the formation flying partner is unavailable and the relative orbit decay can be inferred from the ground track offset relative to a fixed drag-free reference ground track, in Fig.3, the actual ground track offsets for TOPEX/Poseidon "navigation solutions" and POE's agree to better than 40 m. Thus, with similar orbit determination on EO-1 the "navigation solutions" will be adequate to detect drag induced orbit decay. The maneuver decision function describes this process more completely.

Fig. 3 - TOPEX/Poseidon Ground Track History

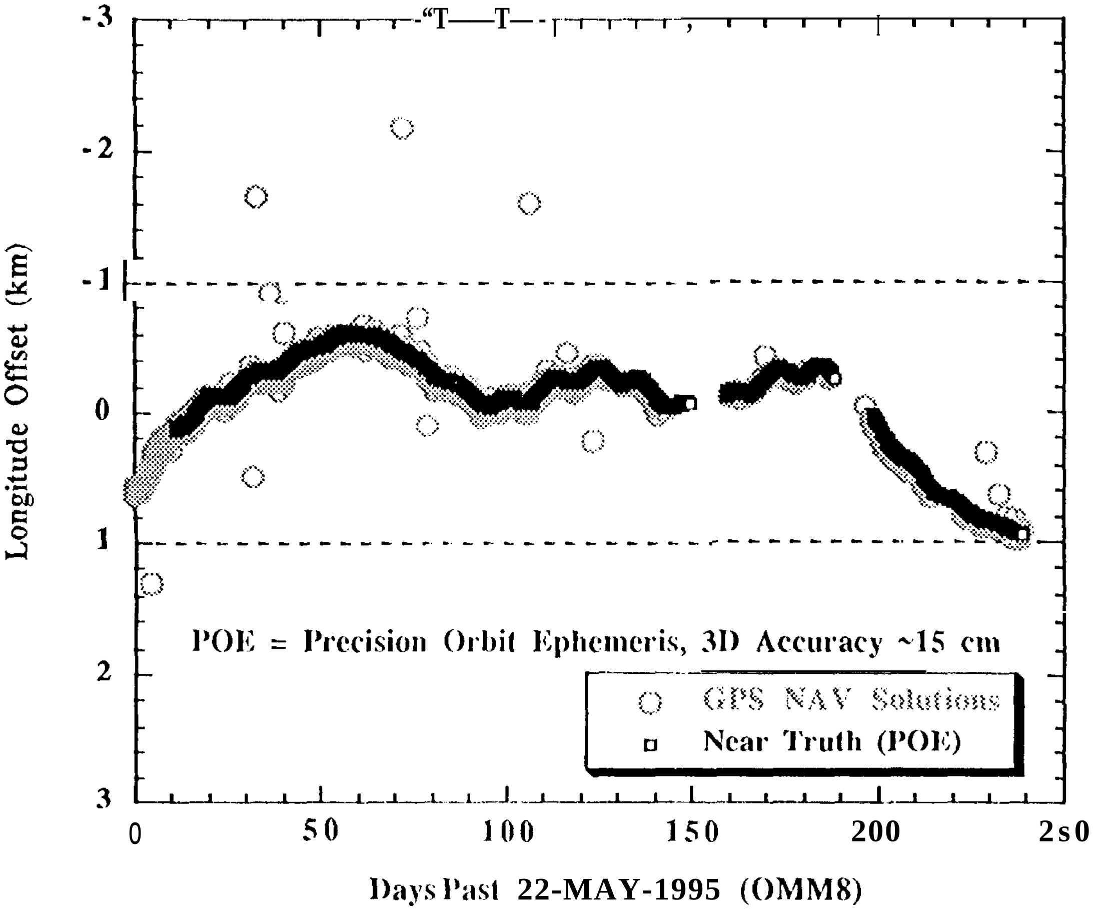

MANEUVER DECISION AND DESIGN

Two types of orbit control maneuvers are required for formation flying. The first are those required to account for variations in the along track separation due to differential atmospheric drag on the formation members. In this paper, these are referred teas Along Track Adjustment Maneuvers (ATAM's). The second are maneuvers that each member of the formation must perform due to individual mission constraints (e.g., ground track maintenance or ground target acquisitions). These second types are called Orbit Maintenance Maneuvers (OMM's). For a cooperative formation flying mission OMM's can be coordinated autonomously through a spacecraft to spacecraft telecommunications link, Since EO-1 will be non-cooperative, the LS-7 OMM's must be provided to EO-1 through a non-autonomous path (e.g., ground uplink). However, with the control strategy described below ATAM's processing can remain completely autonomous,

The primary orbital perturbations, responsible for along track separation variations, are aspherical gravity and atmospheric drag. Both are fundamental in defining the minimum separation control requirements. In this paper, ATAM's only control the along track variations due to atmospheric drag.

A spherical Gravity - Since the Earth's geopotential field is aspherical, there exist periodic along track orbit variations between formation members that vary with the nominal separation distance. Fig.4 shows the amplitude of these variations for the proposed EO-1 orbit at nominal separations up to 6000 km (about 15 minutes). Attempts to control the separation to a level lower than a value obtained from Fig. 4 requires multiple maneuvers every orbital revolution. To avoid this resources expense (i.e., fuel, computational, etc.), knowledge of the gravitational induced periodic variations provides a constraint for the minimum separation control.

Fig. 4- Along Track Varaitions Due to 20x20 Aspherical Gravity

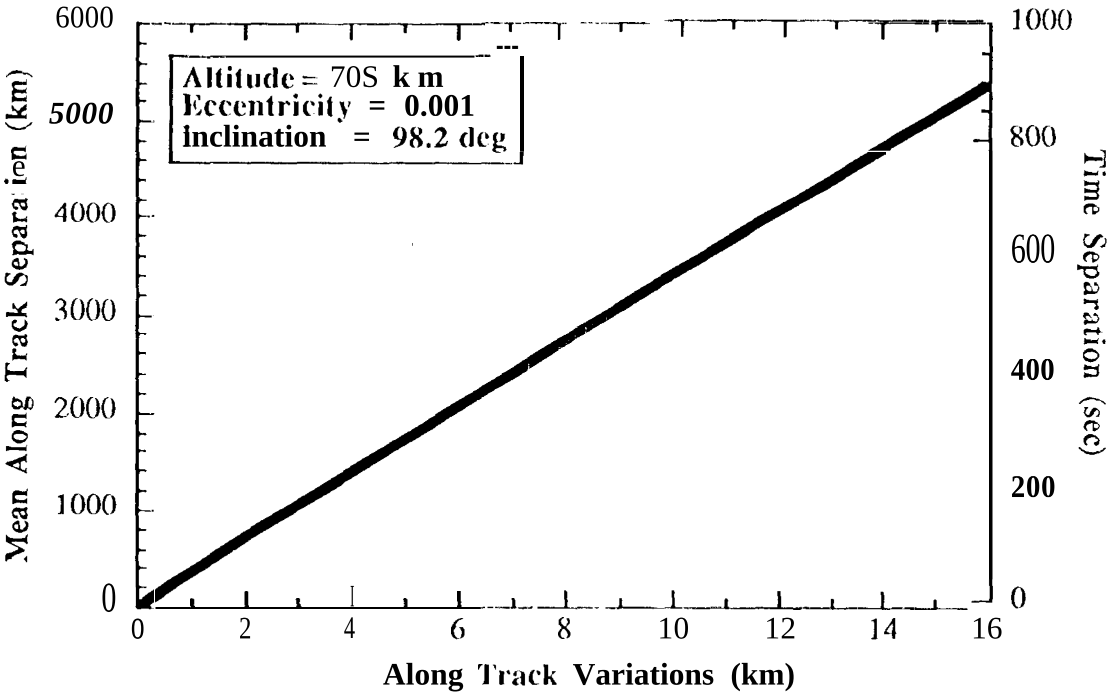

Atmospheric Drag - Non-periodic along track variations arise from the difference in the drag forces acting on each spacecraft. The relative drag accelerations for each spacecraft dictate whether the along track separation wi II increase or decrease. For example, with EO-1 flying in front of 1 .S-7 and having a design such that its drag is higher than that of 1,S-7, the separation will tend to increase (i.e., higher drag on EO-1 lowers its orbit altitude and thus decreases its orbital period compared with I .S-7 and moves away from I .S-7).

A control strategy for computing ATAM's has been developed to account for drag induced behavior of the along track separation. To first order the along track separation between two spacecraft in nearly the same orbit will exhibit quadratic behavior. The relationship is:

$$\mathrm{AA''}]' = \Lambda AT_0 - 2kda_0\, t + k\dot{a}(R-1)\, t^2 \tag{1}$$

where:

ΛAT = along track separation at time t

ΛAT_0 = along track separation at time to

k = orbit constant

da_0 = semimajor axis difference at to

R = ratio of ballistic coefficients

$\dot{a}$ = semimajor axis rate

t = time

Differences in the bal list ic coefficients of each spacecraft (i .e., area-t o-mass ratio multiplied by the drag coefficient) produce differences in the atmospheric drag accelerations on each spacecraft. Mathematically, the difference in the along track orbit angle (mean anomaly) between the two spacecraft, is the quadratic function of time and orbit decay rate shown above in (1) and derived in the Appendix, Once the relative ballistic coefficients and orbit decay are known, this quadratic relationship can be used to extrapolate the along track separation to the control boundaries and thus predict when an ATAM is required.

Orbit decay is characterized by a decrease in the orbital semimajor axis. The semimajor axis decay rate of 1 :O- 1 can be determined directly from the mbit determination process or from an empirical model of the ground track offset history relative to a fixed Cirag-free ground track. The latter method allows for simplified orbit determination. That is, orbit determination accuracies at the 100 m level are adequate for semimajor axis rate determination with a simple empirical model. Without the empirical approach, orbit state accuracies from the orbit determination process are. required to be less than 5 m, thus, requiring the more complex Kalman filtering orbit determination approach.

Semimajor axis decay rates computed directly from the orbit determination process arc obtained by transforming the Cartesian spacecraft states (i.e., positions and velocities) to mean Keplerian elements (i.e., a,e,i,Ω,ω,M). Successive estimates of the semimajor axis (a) provide the decay rate. The simpler empirical model approach produces semimajor axis decay rate information from quadratic fit parameters of the equatorial longitude offsets. For example, Fig.5 shows a quadratic empirical fit to longitude offsets. An estimate of the semimajor axis decay rate can be computed from the m_2 coefficient. This is the basis of single spacecraft autonomous navigation for groundtrack repeat missions[1]. A basic mathematical description for this method can be found in the Appendix.

Fig. 5- Empirical Fit to Equatorial Longitude Offsets

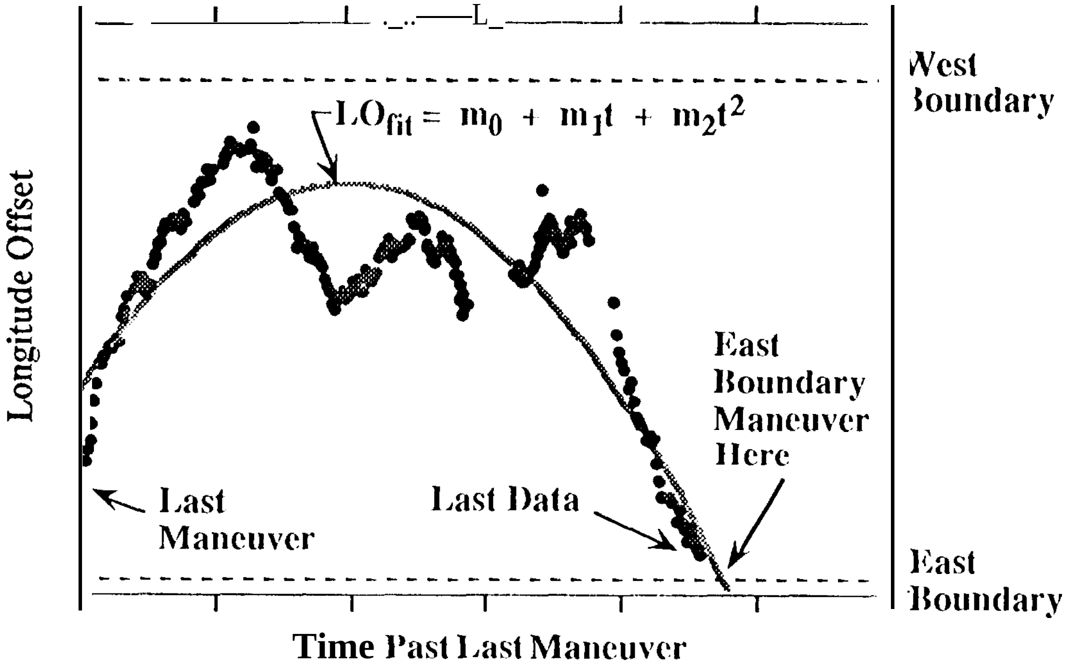

Since the EO-1 mission is non-cooperative, the LS-7 semimajor axis decay rate is not routinely available. Assuming both spacecraft encounter the same atmospheric density the LS-7 semimajor axis decay rate can be derived from the following:

$$\dot a_{LS\text{-}7} = R\dot a_{EO\text{-}1} = \frac{\beta_{EO\text{-}1}}{\beta_{LS\text{-}7}}\dot a_{EO\text{-}1} = \frac{\left(C_D\frac{A}{m}\right)_{EO\text{-}1}}{\left(C_D\frac{A}{m}\right)_{LS\text{-}7}}\dot a_{EO\text{-}1} \qquad (2)$$

where:

$\dot{a}$ = semimajor axis rate
β = spacecraft ballistic coefficient
C_D = spacecraft drag coefficient
A = spacecraft projected area in along track direction
m = spacecraft mass

Once the orbital decay is determined the along track control boundaries can be monitored with equation (1). When a control boundary is exceeded, the magnitude of the ATAM can be computed based on the known difference in semimajor axes between the two spacecraft. ATAM magnitudes are computed with:

$$\Delta V = \frac{4}{3} k da_M \tag{3}$$

where:

ΔV = along track velocity change
k = orbit constant
da_M = semimajor axis difference at maneuver epoch

SIMULATION RESULTS

Simulation results of the EO-1 mission with a nominal along track separation of 900 km (about 2 minutes) forward of LS-7 are presented in this section. The along track control boundary for ATAM's was set at ±10 km. LS-7 ground track boundaries for OMM'S were set at ±5 km. The EO-1 spacecraft ballistic coefficient was assumed to be twice that of LS-7. Figs.6-8 show a simulated history of the EO-1 and LS-7 along track separation, semimajor axes, and equatorial longitude offsets.

The line labeled "Truth" in Fig.6 was computed by differencing the EO-1 and LS-7 fully dynamic trajectories. The per orbit variations show amplitudes of about 2 km that are consistent with Fig.4. Two ATAM's and an OMM were included in the simulation. The semimajor axis of EO - 1 was determined using simulated GPS "navigation solutions" and the empirical method described earlier in this paper. in Fig.7 the semimajor axis results reveal some observability problems at the beginning of each segment fit by the empirical model. This initialization problem can be handled with some apriori constraints and is not expected to impair the empirical method. **Fig.8 shows** very good agreement between the actual ground tracks of EO-1 and LS-7. This shows the most important result since the EO-1 spacecraft is required to co-image the same geographical locations as LS-7.

Fig. 6 - Along Track Variations

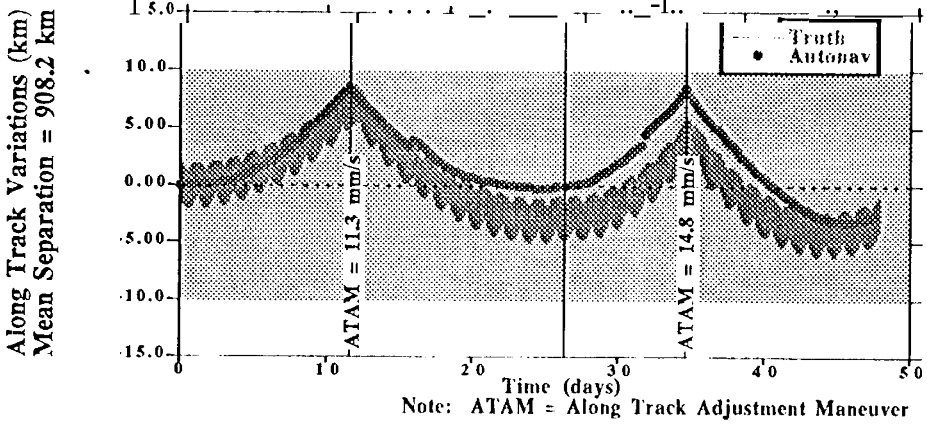

Note: ATAM = Along Track Adjustment Maneuver

Fig. 7- Semimajor Axis Variations

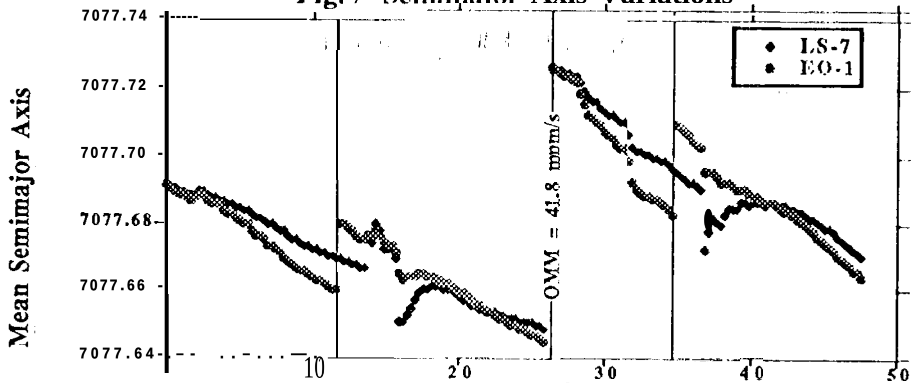

Note: OMM = Orbit Maintenance Maneuver

Fig. 8- Ground Track Variations

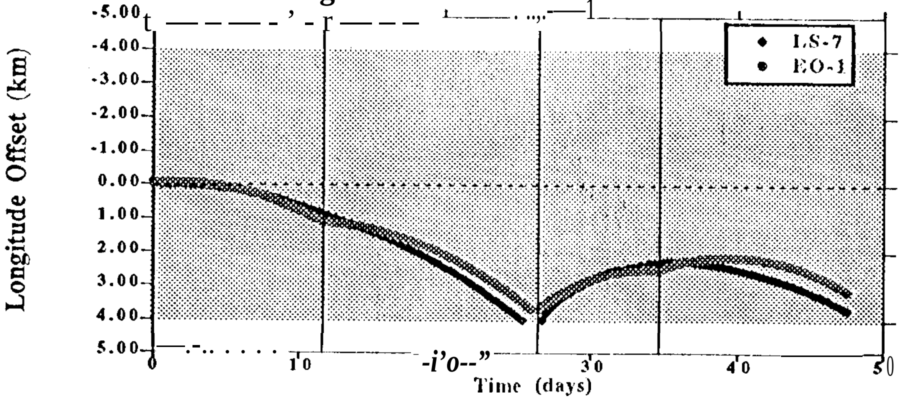

RESOURCE REQUIREMENTS

Autonomous navigation for formation flying on EO-1 is implemented fundamentally as flight software hosted either in the satellite Command and Data Handling (GQIJ11) computer or in a dedicated computer with interfaces to the C&DH computer. (Preliminary estimates indicate that a dedicated computer could be provided for ≈5 kg and ≈15 watts.) Whichever computer is used, it needs to provide ≈400 Kbytes of memory and processing speeds of up to ≈10 MIPS. in addition, autonomous formation flying needs a GPS receiver to provide tracking data, This capability is assumed to be included nominally within the spacecraft. This GPS technology is the same technology that will be the basis of future missions addressing more strenuous, more accurate forms of formation flying under different mission scenarios and with different navigation requirements.

Fuel usage is expected to increase at most about 2.S% over the baseline design. Nominally, the EO-1 mission will fly for 12 to 18 months in the latter part of this decade. Considering the expected maximum solar activity (i.e., largest expected drag) the baseline fuel budget for 1 S-'7 is about 3 m/s for OMM's only [20]. Assuming atmospheric drag on HO- I is twice that of 1.S-7 the EO-1 maneuver fuel budget would be 6 m/s. Adding formation flying, the total maximum fuel budget for EO-1 ATAM's and OMM'S is 7.5 m/s.

VALIDATION

Regarding the plan for validating this technology, formation flying algorithms would first be verified by detailed simulations of the autonomous navigation system within ground-based computers to determine their robustness and resiliency to various nominal and off-nominal conditions. Subsequently, flight software versions of these algorithms would be tested and used to simulate in a ground-based real.-time simulation the two satellites flying in formation, i.e., in some sort of testbed. Then, after launch and system calibration, e.g., especially the differences in the ballistic coefficients between EO-1 and IS-7, the autonomous navigation system would be activated in steps to perform formation flying, but with continuous ground monitoring of the performance. For example, it might be determined that a maneuver execution experiment like the TOPEX/POSEIDON Autonomous Maneuver Experiment (TAME) [21] would be a prudent test of the Maneuver Implementation Function software without fully committing to autonomous operations. Regardless, validation is dine. step by step, and only after a Flight Readiness Review of the autonomous navigation system, looking at actual on-orbit performance, would the system be activated in a truly autonomous mode. Even then, ground-based analysts would monitor performance through two or three maneuvers before the staff would be reduced and the system pronounced sound.

CONCLUSIONS

In conclusion, the benefit of this technology and its demonstration on EO-1 is ultimately the elimination of ground operators who would be required to determine command sequences for a series of orbit adjustment/maintenance maneuvers driven by the changing environment. Additionally, with autonomous navigation, the satellite will inherently know where it is (orbit determination), where it will be in the future (orbit prediction), and how to change its state to assure that it gets to where it is required to be, all without human decision making or ground intervention. Eventually, this could lead to a series of "virtual platforms" all flying in formation taking coordinated measurements for Mission to Planet Earth science.

ACKNOWLEDGEMENTS

The research described in this paper was carried out by the Jet Propulsion Laboratory, California Institute of Technology, under contract with the National Aeronautics and Space Administration.

REFERENCES

[1] Guinn, J. R., and others, "Autonomous Spacecraft Navigation for Earth Ground Track Repeat Orbits Using GPS," presented at the AAS/AIAA Space Flight Mechanics Meeting, Austin, TX., 12-15 February 1996,

[2] Wertz, J.R., "Implementing Autonomous Orbit Control," presented at the 19th Annual AAS Guidance and Control Conference, Breckenridge, CO., 7-11 February 1996.

[3] Collins, J., and R. Conger, "MANS: Autonomous Navigation and Orbit Control for Communications Satellites," AIAA 94-1127-CP, presented at the AIAA International Communication Satellite Systems Conference, San Diego, CA., 15 February 1994.

[4] Ketchum, E., "Autonomous Spacecraft Orbit Determination Using Magnetic Field and Attitude information," presented at the 19th Annual AAS Guidance and Control Conference, Breckenridge, CO., 7-11 February 1996.

[5] Anthony, J. and P. Pepperi, "U.S. Air Force Phillips Laboratory Autonomous Space Navigation Experiment," presented at the AIAA/Utah State University Conference on Small Satellites, September 1992.

[6] Gramling, C. J., and others, "Flight Qualification of the TDRSS Onboard Navigation System (TONS)," presented at the AAS/AIAA Astrodynamics Specialists Conference, Victoria, B. C., Canada, 16-19 August 1993.

[7] Clohessy, W. and R. Wiltshire, "Terminal Guidance System for Satellite Rendezvous," *Journal of the Aerospace Sciences*, Vol. 27, No. 9, pp. 653-658, Sept., 1960.

[8] Vassar, R. and R. Sherwood, "Formationkeeping fot a Pair of Satellites in a Circular Orbit," *Journal of Guidance, Control, and Dynamics*, Vol. 8, No. 2, pp. 235-2.42, Mar-Apr, 1985.

[9] Middour, J. W., “Along Track Formationkeeping for Satellites with Low Eccentricity,” *Journal of the Astronautical Sciences*, Vol. 41, No. 1, pp. 19-33, Jan-Mar, 1993.

[10] Wu, S.C., and others, “MicroGPS for Orbit Determination of Earth Satellites,” to be published in the Institute of Navigation Proceedings of 1996 National Technical Meeting, April, 1996.

[11] Parkinson, B.W., “Introduction and Heritage of NAVSTAR, the Global Positioning System,” Global Positioning System: Theory and Applications, Vol. 1, pp 3-28, Progress in Astronautics and Aeronautics, Vol. 163, 1996.

[12] Meehan, T., and others, “The TurboRogue GPS Receiver,” presented at the Sixth International Geodetic Symposium on Satellite Positioning, Columbus, OH., 18 March 1992.

[13] van Grass, F, and M. Braasch, “Selective Availability,” Global Positioning System: Theory and Applications, Vol. 1, pp 3-28, Progress in Astronautics and Aeronautics, Vol. 163, 1996.

[14] 1992 Federal Radionavigation Plan, DOT-VNTSC-RSPA-92-2/DOD-4650.5.

[15] Bertiger, W., et al., GPS precise tracking of TOPEX/POSEIDON: Results and implications, *J. Geophys. Res.*, 99, 2.4449-2.4464, 1994.

[16] Heuberger, J., and L. Church, “Landsat-4 Global Positioning System Navigation Results,” AAS 83-363, Proceedings of the American Astronomical Society/AIAA Astrodynamics Conference, Lake Placid, NY., Aug 22-25, 1983.

[17] Guinn J. and others, “TAOS Orbit Determination Results Using Global Positioning Satellites,” AAS-95-146, presented at the AAS/AIAA Spaceflight Mechanics Meeting, Albuquerque, New Mexico, 13-16 February 1995.

[181 Meehan, T., and others, “The GPS/MET Atmospheric Occultation Receiver,” presented at the American Geophysical Union Fall Meeting, San Francisco, CA., 1995.

[19] Bertiger, W., and others, “Single Frequency GPS Orbit Determination for Low Earth Orbiters,” to be published in the Institute of Navigation Proceedings of 1996 National Technical Meeting, April, 1996.

[20] LANDSAT 7 Space Segment Satellite Critical Design Review, Lockheed Martin presentation material, October 10-11, 1995.

[21] Kia, T., and others, “Topex/Poseidon Autonomous Maneuver Experiment (TAME),” presented at the 19th AAS Guidance and Control Conference, Breckenridge, CO., 7-11 February 1996

[22] Frauenholz, R, R. Bhat, E. Cannell, “Estimates of Velocity Magnitude and Timing for TOPEX Drag Make-up Maneuvers,” JPL IOM (internal document) 314.4-12.67, 19 May 1988.

Appendix - Mathematical Derivations

This appendix is provided to document the derivation of an empirical method for determining the semimajor axis rate and using Ibis information for maneuver decision and design functions. Portions of the following were originally described in Ref.22.

To understand how a change in the along track velocity effects the along track position we start with Kepler's equation:

$$M = E - e\sin E = n(t - t_p) \tag{A1}$$

where: M = mean anomaly
E = eccentric anomaly
e = eccentricity
n = mean motion
t = time
t_p = time past periapsis

For circular orbits and $M_0 = -nt_p$ equation A 1 becomes

$$M = E = M_0 + nt \tag{A2}$$

The along track velocity is:

$$V = \sqrt{\frac{\mu}{a}} \quad \text{circular velocity} \tag{A3}$$

where: μ = Earth gravitational constant
a = spacecraft semi-major axis

From equation A3, a change in semi-major axis yields a change in velocity as follows:

$$dV = -\frac{V}{2a}\,da \tag{A4}$$

From Kepler's third law:

$$n = \sqrt{\frac{\mu}{a^3}} \quad \text{mean motion} \tag{A5}$$

Equations A3 and A5 can be combined to show how a change in semi-major axis results in a change in the mean motion:

$$dn = -\frac{3n}{2a}\,da \qquad \text{(A6)}$$

The change in mean anomaly due to a change in the along track velocity can now be derived from equations A1, A4, and A6:

$$AM = (dn)\,t = 3n\frac{dV}{V}\,t \ \text{(no atmospheric drag)} \qquad \text{(A7)}$$

Adding atmospheric drag, equation A7 becomes:

$$AM = (dn)\,t + \frac{\dot{n}}{2}t^2 \qquad \text{(A8)}$$

The time derivative of the mean motion is:

$$\dot{n} = -\frac{3n}{2a}\,\dot{a} \qquad \text{(A9)}$$

And for a circular orbit the atmospheric drag effect on semi-major axis is:

$$\dot{a} = -\frac{C_D A}{m}\,\frac{\rho V^2}{n} \qquad \text{(A10)}$$

where: C_D = spacecraft drag coefficient
A = spacecraft projected area in along track direction
m = spacecraft mass
p = atmospheric density

Combining equations A7-A10 the along track angular change due to an along track velocity increment and atmospheric drag decay is:

$$AM = \left(3n\frac{dV}{V}\right)t + \left(\frac{3}{4}\,\frac{C_D A}{m}\,\rho V n\right)t^2 \qquad \text{(A11)}$$

The along track distance computed from the along track angular change is:

$$AT = a\,AM \qquad \text{(A12)}$$

A change in orbital period due to a change in along track distance is:

$$AT = \frac{AT}{V} \qquad \text{(A13)}$$

Finally, the angular change in equatorial longitude is:

$$\Delta\lambda = \Delta\lambda_0 + \omega_e \Delta T = \Delta\lambda_0 + \omega_e \frac{a\Delta M}{V} \tag{A14}$$

Substituting equation A11 into A14 gives:

$$\Delta\lambda = \Delta\lambda_0 + \left(\frac{3\omega_e}{V} dV\right) t + \left(\frac{3}{4}\omega_e \frac{C_D A}{m} \rho V\right) t^2 \tag{A15}$$

Rewriting in terms of semi-major axis rate (i.e., using equation A 10)

$$\Delta\lambda = \Delta\lambda_0 + \left(\frac{3\omega_e}{V} dV\right) t - \left(\frac{3\omega_e}{4a} \dot{a}\right) t^2 \tag{A16}$$

Next, convert the angular longitude offset to a length measurement as:

$$LO = a_e \Delta\lambda \tag{A17}$$

where: a_e = Earth mean equatorial radius

The final expression for the ground track longitude offset is then:

$$LO = LO_0 + \left(\frac{3\omega_e a_e}{V} dV\right) t - \left(\frac{3\omega_e a_e}{4a} \dot{a}\right) t^2 \tag{A18}$$

Now, the equation for a quadratic fit to LO is:

$$LO = m_0 + m_1 t + m_2 t^2 \tag{A19}$$

Therefore, the initial longitude offset, velocity change and semi-major axis rate in terms of the quadratic fit coefficients can be determined from equations A18 and A19 as:

$$LO_0 = m_0 \tag{A20}$$

$$dV = \frac{V m_1}{3\omega_e a_e} \tag{A21}$$

$$\dot{a} = -\frac{4a m_2}{3\omega_e a_e} \tag{A22}$$

With the semimajor axis rate determined from A22, the along track separation can be computed. First, the angular difference between the mean anomalies of two spacecraft (EO-1 and LS-7) is computed from equations A2 and A8:

$$\Delta D = \left(M_{EO\text{-}1} + \Delta M_{EO\text{-}1}\right) - \left(M_{LS\text{-}7} + \Delta M_{LS\text{-}7}\right) \qquad (A23)$$

The along track distance is:

$$AAT = aAD \qquad (A24)$$

Nominally $\Delta M_0 = M_{EO\text{-}1} - M_{LS\text{-}7}$, so A24 becomes:

$$\Delta AT = a\,A\,M_o + a\left(\Delta M_{EO\text{-}1} - \Delta M_{LS\text{-}7}\right) \qquad (A25)$$

Expanding A25 as in equation A11:

$$AAT = \Delta AT_0 + 3(dV_{EO\text{-}1} - dV_{LS\text{-}7})\,t - k(\dot{a}_{EO\text{-}1} - \dot{a}_{LS\text{-}7})\,t^2 \qquad (A26)$$

where: k = orbit constant = $3V/4a$

For the same atmospheric density and semimajor axis the following holds:

$$R = \frac{\beta_{LS\text{-}7}}{\beta_{EO\text{-}1}} = \frac{\dot{a}_{LS\text{-}7}}{\dot{a}_{EO\text{-}1}} \qquad (A27)$$

incorporating equations A4 and A27 into A26 gives the along track separation as a function of time, the initial along track separation, the initial semimajor axis difference and the semimajor axis time rate of change of only one of the spacecraft.

$$AAT = \Delta AT_0 - 2k\,da_0\,t + k\dot{a}_{EO\text{-}1}(R-1)\,t^2 \qquad (A28)$$

Maneuver magnitudes are chosen to target the opposite along track boundary by doubling the semi major axes difference at the maneuver epoch. Thus, maneuver magnitudes can be computed from A4 as follows:

$$\Delta V = \frac{4}{3}k\,da_M \qquad (A29)$$

where: AV = along track velocity change
k = orbit constant = 3V/4a
da_M = semimajor axis difference at maneuver epoch